



ORIGINAL ARTICLE

Histological sequence of the development of rat mesothelioma by MWCNT, with the involvement of apolipoproteins

Motoki Hojo¹  | Yukio Yamamoto¹ | Yoshimitsu Sakamoto¹ | Ai Maeno¹ | Aya Ohnuki¹ | Jin Suzuki¹ | Akiko Inomata¹ | Takako Moriyasu¹ | Yuhji Taquahashi² | Jun Kanno² | Akihiko Hirose² | Dai Nakae³ 

¹Department of Pharmaceutical and Environmental Sciences, Tokyo Metropolitan Institute of Public Health, Tokyo, Japan

²Center for Biological Safety and Research, National Institute of Health Sciences, Kanagawa, Japan

³Department of Nutritional Science and Food Safety, Faculty of Applied Biosciences, Tokyo University of Agriculture, Tokyo, Japan

Correspondence

Dai Nakae, Department of Nutritional Science and Food Safety, Faculty of Applied Biosciences, Tokyo University of Agriculture, 1-1-1 Sakura-ga-Oka, Setagaya, Tokyo 156-8502, Japan.
Email: agalennde.dai@nifty.com

Funding information

Ministry of Health, Labour and Welfare, Grant/Award Number: H27-Kagaku-Shitei-004 and H30-Kagaku-Shitei-004

Abstract

A rat model of mesothelioma development by peritoneal injection of multiwalled carbon nanotube (MWCNT) has been established and found to be useful to understand the mechanisms underlying fibrous particles-associated carcinogenesis. Its detailed histological sequence, however, remains largely obscure. We therefore aimed to assess the time-course of mesothelioma development by MWCNT and evaluate a set of lipoprotein-related molecules as potential mechanism-based biomarkers for the phenomenon. Male Fischer 344 rats were injected intraperitoneally (ip) with MWCNT (MWNT-7) at 1 mg/kg body weight, and necropsied at 8, 16, 24, 32, or 42 wk after injection. For biochemical analyses of the lipoprotein-related molecules, more samples, including severe mesothelioma cases, were obtained from 2 other carcinogenicity tests. Histologically, in association with chronic inflammation, mesothelial proliferative lesions appeared at c. Wk-24. Before and at the beginning of the tumor development, a prominent infiltration of CD163-positive cells was seen near mesothelial cells. The histological pattern of early mesothelioma was not a papillary structure, but was a characteristic structure with a spherical appearance, composed of the mesothelioma cells in the surface area that were underlain by connective tissue-like cells. Along with the progression, mesotheliomas started to show versatile histological subtypes. Serum levels of apolipoprotein A-I and A-IV, and a ratio of HDL cholesterol to total cholesterol were inversely correlated with mesothelioma severity. Overall, the detailed histological sequence of mesotheliomagenesis by MWCNT is demonstrated, and indicated that the altered profile of apolipoproteins may be involved in its underlying mechanisms.

KEYWORDS

apolipoprotein, cholesterol, MWCNT, peritoneal mesothelioma, rat

Abbreviations: Apo, apolipoprotein; CTGF, connective tissue growth factor; HDL, high density lipoprotein; H-T ratio, ratio of HDL cholesterol and total cholesterol; LDL, low density lipoprotein; L-T ratio, ratio of LDL cholesterol and total cholesterol; MPM, malignant pleural mesothelioma; MWCNT, multiwalled carbon nanotube; PLF, peritoneal lavage fluid.

This is an open access article under the terms of the Creative Commons Attribution-NonCommercial-NoDerivs License, which permits use and distribution in any medium, provided the original work is properly cited, the use is non-commercial and no modifications or adaptations are made.

© 2021 The Authors. *Cancer Science* published by John Wiley & Sons Australia, Ltd on behalf of Japanese Cancer Association.

1 | INTRODUCTION

The development and application of multiwalled carbon nanotubes (MWCNT) have proliferated over the last 2 decades, as a result of their promising mechanical, thermal, chemical, and electrical properties. These advantages will allow the expansion of MWCNT from their current, relatively limited uses in the electronics and medical fields, to more ubiquitous uses, for instance in cars and electrical distribution systems. Following this expansion, substantial waste discharge is expected that would be finally emitted into the air. The asbestos-like fibrous structure and highly bio-persistent features of MWCNT are therefore of great concern. Intensive long-term toxicological studies have unveiled the chronic or subchronic toxicities of MWCNT, such as fibrosis and tumors in the lung.¹⁻⁴ In particular, 2 carcinogenicity studies using Fischer 344 rats and *p53*-heterozygously knocked-out C57BL/6 mice have clearly indicated the risk for the development of mesothelioma.^{5,6} It has recently been shown that MWCNT can induce pleural mesothelioma in rats after repeated intratracheal administrations.^{4,7}

It is assumed that biological undegradable fibers can cause damage directly or indirectly to the DNA of mesothelial cells, for example *cdkn-2a/2b* deletion, and also activate pro-inflammatory cytokine secretions mainly by from fiber-engulfing macrophages in a state of "frustrated phagocytosis," both of which can lead to a neoplastic condition.⁸⁻¹¹ However, there is a paucity of data describing chronological change during mesotheliomagenesis of MWCNT. This information is essential to understand the early phase of tumorigenesis, and will contribute not only to the design and evaluation of chronic toxicity tests for fibrous nanomaterials, but also to finding early biomarkers or therapeutic targets for human malignant pleural mesothelioma (MPM).

The purpose of this study was to investigate the histological sequence of mesothelioma development caused by MWCNT. In addition, using a large spectrum of pathological data on the mesothelium, ranging from non-neoplastic lesions to severe mesotheliomas, we analyzed a set of lipoprotein-related molecules in the blood samples to explore their possible use as potential biomarkers for the generation of mesothelioma. This is because, in our preliminary proteomic analysis for rat peritoneal mesotheliomagenesis by MWCNT, apolipoprotein A-IV (Apo A-IV) was found to be a candidate (data not shown).

2 | MATERIALS AND METHODS

2.1 | Animal treatments and preparation of MWCNTs

Male F344/DuCrj (Fischer 344) rats were purchased from Charles River Laboratories (Kanagawa, Japan), maintained at a temperature of 23°C and 45% relative humidity under a 12-h light-dark cycle. Animals were given a basal diet, CE-2 (CLEA Japan, Tokyo, Japan), and tap water ad libitum, and housed in polycarbonate cages (3 rats per cage).

Suspensions of MWCNT or vehicle were injected ip to rats at a volume of 1 mL/kg body weight (BW). MWCNT suspensions were

prepared as described below and sonicated using an ultrasound bath (150 W) for 30 min immediately before the administration.

Experiment 1: For the time-course analysis, MWNT-7 (6.65 μ m in length and 66.8 nm in diameter; a gift from Mitsui Chemicals, Tokyo, Japan; Figure S1) was suspended into a 2% carboxymethyl cellulose (CMC) solution. In total, 48 rats were dosed with 1 mg/kg BW of MWNT-7 at 8 wk of age and sacrificed and necropsied sequentially at 8, 16, 24, or 32 wk after injection (8, 12, 14, or 14 animals, respectively; sequential necropsies test). In addition, 12 rats were dosed at 12 wk of age and maintained for 42 wk after injection (carcinogenicity assessment test). The vehicle controls were similarly treated in both tests (40 and 10 rats in sequential necropsies and carcinogenicity assessment tests, respectively) (Figure S1).

Experiment 2: A 2-y test with a different dosage setting was performed to obtain a data set of rats with varying degrees of mesothelioma. Taquann-MWNT-7 (Taq-MWNT-7) was prepared using the "Taquann" method to remove large agglomerates of fibers.¹² Both Taq-MWNT-7 and original MWNT-7 were dispersed into physiological saline containing 0.1% Tween-80. Next, 10-wk-old rats were divided into 4 groups and injected with one of the following doses: vehicle, 0.05 mg/kg BW of Taq-MWNT-7, 1 mg/kg BW of Taq-MWNT-7, or 1 mg/kg BW of original MWNT-7. Animals were maintained for 104 wk after injection (Figure S4).

Experiment 3: Specimens were obtained from a previous study in which 7 different types of carcinogenic MWCNTs (MWNT-7, N, T, SD-1, SD-2, WL, and WS) were evaluated¹³ to analyze rats treated with different MWCNTs. Briefly, 10-wk-old rats were dosed with the vehicle or 1 mg/kg BW of each MWCNT, and the terminal sacrifice was conducted at 52 wk after injection. This time was chosen because we confirmed that a positive control fiber (MWNT-7) can induce mesothelioma in 100% of rats in a year at this dosage. Among the samples in this study, histological slides and sera from the 3 groups (vehicle, SD-1 [carcinogenic fiber; long and thick], and SD-2 [non-carcinogenic fiber; tangled and thin]) were used for analysis.

At the periodical sacrifices and at termination of the experiments, animals were killed by exsanguination through the abdominal aorta under isoflurane anesthesia. Animals that were moribund or died before the study termination were similarly examined.

Experimental protocols were approved by the Experiments Regulation Committee and the Animal Experiment Committee of the Tokyo Metropolitan Institute of Public Health.

2.2 | Pathology

All rats were weighed and examined macroscopically over all the body, including celomic cavities when autopsied. All major organs and other tissues, such as the mesenterium were resected, fixed in 10% neutrally buffered formalin, processed routinely to prepare paraffin-embedded sections and stained with hematoxylin and eosin (H&E). The mesothelium of the entire abdominal cavity was assessed using a pathological grading method ("Total Consecutive Grade"; 0-8) (Table 1). Rats with no or minimal changes were assigned as 0. Under conditions with no

TABLE 1 Pathological grading criteria of abdominal lesions

Diagnosis		Gross and microscopic findings	Total Consecutive Grade
No change		No or minimal change.	0
Inflammation	Weak	Minimal infiltration of inflammatory cells with frequent finding of the deposition of MWCNT-laden macrophages at the lymphatic infiltration of the peritoneum. No reactive change on mesothelial cells.	1
	Intermediate	Frequent findings of edematously thickened mesothelium with fibrosis. Infiltrations of eosinophil, monocyte, macrophage, and mast cell.	2
	Strong	Marked infiltration of monocytes and reactively proliferated mesothelial cells in the surface of the mesothelium.	3
Hyperplasia		Protrusion of several layers of enlarged mesothelial cells accompanied with rich connective tissue-like cells. Occasional appearance of atypical mesothelial cell bulging or mitotic figures.	4
Mesothelioma	Grade-1	Fine nodules or protrusion on the surface of the serosa, grossly recognizable but not so marked. No invasion or metastasis.	5
	Grade-2	Small nodules larger than 1 mm in diameter throughout the coelom. Thickness of the plaque-like tumor mass less than 3 mm on the diaphragm.	6
	Grade-3	Wide distribution of tumor nodules in the coelom including the scrotum. A few large nodules more than 10 mm. Thickness of the plaque-like tumor mass more than 3 mm on the diaphragm.	7
	Grade-4	Large tumors (nodule/mass and thick plaques) occupied the coelom. A few huge nodules at least more than 10 mm with some being 20-30 mm. More than 10 of nodules with large (more than 10 mm) or middle (5-10 mm) sizes, or thick plaque more than 3 mm covering throughout the serosa. Tumor invasion surrounding tissues including digestive tract wall, the parenchyma of liver, kidney, spleen, and the coelomic walls.	8

proliferative lesions, animals were given a grade from 1 to 3 in accordance with the inflammation level. Once the proliferative lesion occurred, which could be recognized as the pathological phase transition, the rats were given a grade from 4 to 8, in accordance with the proliferative lesions regardless of the inflammatory status (Table 1 and Figures S2 and S3). Each grade from the Total Consecutive Grade from 5 to 8 corresponded to Tumor Grades 1 to 4. The tumor grade was assessed in accordance with the degree of extension of the tumor mass in the peritoneal cavity (Table 1). Mesotheliomas were classified into 3 types (epithelioid [E], sarcomatoid [S], and biphasic [B]) and subtypes in accordance with diagnosis for human MPM.^{14,15} Subtypes of epithelioid mesotheliomas showing solid, signet ring, pleomorphic, and rhabdoid structures were denoted as Esol, Esig, Eple, and Erha, respectively. Sarcomatoid mesotheliomas showing conventional, osteosarcomatous, chondrosarcomatous, desmoplastic, and pleomorphic structures were denoted as Scon, Sost, Scho, Sdes, and Sple, respectively. In Experiment 1, various inflammatory findings in the serosa of the fat tissue surrounding the pancreas were assessed and scored as follows: 0, no, or minimal; 1, slight; 2, moderate; or 3, severe.

For immunohistochemical staining, antigen retrieval was performed using a microwave followed by inactivation of endogenous peroxidase. After blocking, the sections were treated with primary antibodies (Table S1). Diaminobenzidine signals were detected with a horseradish peroxidase-secondary antibody conjugate (K4061; Agilent Technologies, Santa Clara, CA, USA).

Colloidal iron staining and Sirius red staining were performed in accordance with standard protocols.

2.3 | Biochemical analyses of peritoneal lavage fluid and serum

In Experiment 1, the peritoneal cavities of all rats were perfused with 10 mL phosphate buffer (pH 7.4) and retrieved as peritoneal lavage fluid (PLF). In the 3 experiments, sera were obtained from all surviving rats. Humoral factors in these samples were analyzed by ELISA in accordance with the manufacturer's procedures (Table S2). The sera were also examined for total cholesterol, high density lipoprotein (HDL) cholesterol, low density lipoprotein (LDL) cholesterol and triglyceride using an automatic analyzer (TBA-120FR, Canon Medical Systems, Tochigi, Japan).

2.4 | Statistics

Comparisons of values between the 2 different groups were analyzed by Mann-Whitney *U* test. Comparisons of values in multigroup were analyzed by Steel-Dwass test. Trends for ordered change were analyzed by the Jonckheere trend test. Correlations of the 2 variables were analyzed by Spearman test. Differences in values were deemed statistically significant when *P*-values were less than .05.

3 | RESULTS

3.1 | Histological change of the mesothelium before the beginning of mesotheliomagenesis

In Experiment 1, chronic inflammation was observed in association with the gradual formation of mesothelial proliferative lesions (Tables 2 and 3). At the end of week 8 (Wk-8), a large part of administered MWCNT has already been encapsulated within huge granulomas containing many fibrotic elements and macrophages (Figure 1A-C). These granulomas were found preferentially at the rostral region of the abdominal cavity (ie, around the diaphragm, liver, stomach, and pancreas), compared with the caudal region, suggesting a unidirectional clearance of MWCNTs in the peritoneal space. For all examined time points, fibrosis was often observed in the peritoneum. Thick collagenous sheets were observed in the abdominal organ surface, such as the liver and stomach, and the serosa attaching the fat tissues as scars (Figure 1D). In addition, other fibrotic regions were associated with inflammatory lesions of edematous thickenings of the mesothelium, containing free MWCNT fibers or those engulfed by macrophages, and various inflammatory cells such as lymphocytes, eosinophils, monocytes, and mast cells (Figure 1B, E and Table 3). These inflammatory foci were observed constantly from Wk-8 to Wk-24, and some were found near the proliferative changes around Wk-24, which was in contrast with observations that granuloma and the scars site were separate from proliferative lesions. On the surface of these lesions, a population of monocytes (or macrophages) covered the serosa instead of mesothelial cells (Figure 1E). This "monocyte covering" lesion was most often found at Wk-16 (Table 3) and, subsequently, in association

with this finding, enlarged and seemingly regenerative mesothelial cells became prevalent (Figure 1F). From Wk-24, these inflammations gradually subsided, and the growth of submesothelial connective tissue-like (fibroblast-like) cells (Figure 1G) became prominent instead (Table 3). Hyperplasia was first observed at Wk-24 as a protrusion of 2- or 3-layered atypical mesothelial cells accompanied by a proliferation of the submesothelial connective tissue-like cells

TABLE 3 Histological findings of inflammatory changes in the MWCNT-dosed group in the sequential necropsies test in Experiment 1

	Wk-8 (N = 7) ^a	Wk-16 (N = 11)	Wk-24 (N = 14)	Wk-32 (N = 13)
Infiltration of leukocyte	2.3 ± 0.5 ^b	1.9 ± 0.5	1.6 ± 0.8	1.0 ± 0.4 ^c
Edema	2.4 ± 0.5	1.2 ± 0.8	1.5 ± 0.5	0.9 ± 0.5 ^c
Fibrosis	1.9 ± 0.7	2.6 ± 0.5	1.7 ± 0.7	1.6 ± 0.9 ^c
Granulation	2.1 ± 0.9	2.6 ± 0.5	1.9 ± 0.6	2.0 ± 0.6
"Monocyte covering"	1.9 ± 0.9	2.3 ± 0.8	2.1 ± 0.9	0.6 ± 0.7 ^c
Growth of connective tissue-like cell	0	0	0.6 ± 0.9	1.5 ± 0.9 ^d

^aEffective number of rats.

^bMean ± standard deviation of the severity score (see Materials and Methods) in each group.

^cSignificant tendency of decrease from Wk-8 to Wk-32.

^dSignificant tendency of increase from Wk-8 to Wk-32.

TABLE 2 Pathological grading of each rats in the MWCNT-dosed group in Experiment1

		Wk-8 (N = 7) ^a	Wk-16 (N = 11)	Wk-24 (N = 14)	Wk-32 (N = 13)	Wk-42 incl. moribund/dead (N = 11)
Inflammation	Weak	0	0	0	0	0
	Intermediate	5 ^b	3	5	0	0
	Strong	2	8	4	0	0
Hyperplasia		0	0	4	7	1
Mesothelioma	Grade-1	0	0	0	4	2
	Grade-2	0	0	1	1	2
	Grade-3	0	0	0	1	2
	Grade-4	0	0	0	0	4

^aEffective number of rats.

^bNumber of rats bearing lesion.

FIGURE 1 Representative histology of the serosa and the fat tissue around the pancreas before the tumor formation. Edematous thickening with granulomas (A, B, and C), fibrosis (D), and infiltration of leukocytes (E). Reactive proliferation of mesothelial cells (F) and submesothelial cells (G) in the inflammatory lesions. Hyperplasia of the mesothelium with active growth of submesothelial connective tissue-like cells (H, I, and J). Immunohistochemical staining of CD163 (B₁, C₁, E₁, F₁, and J₁), CD68 (C), and mesothelin (B₂, E₂, F₂, I, and J₂). Arrows show MWCNT fibers. Brackets show the growth areas of the connective tissue-like cell

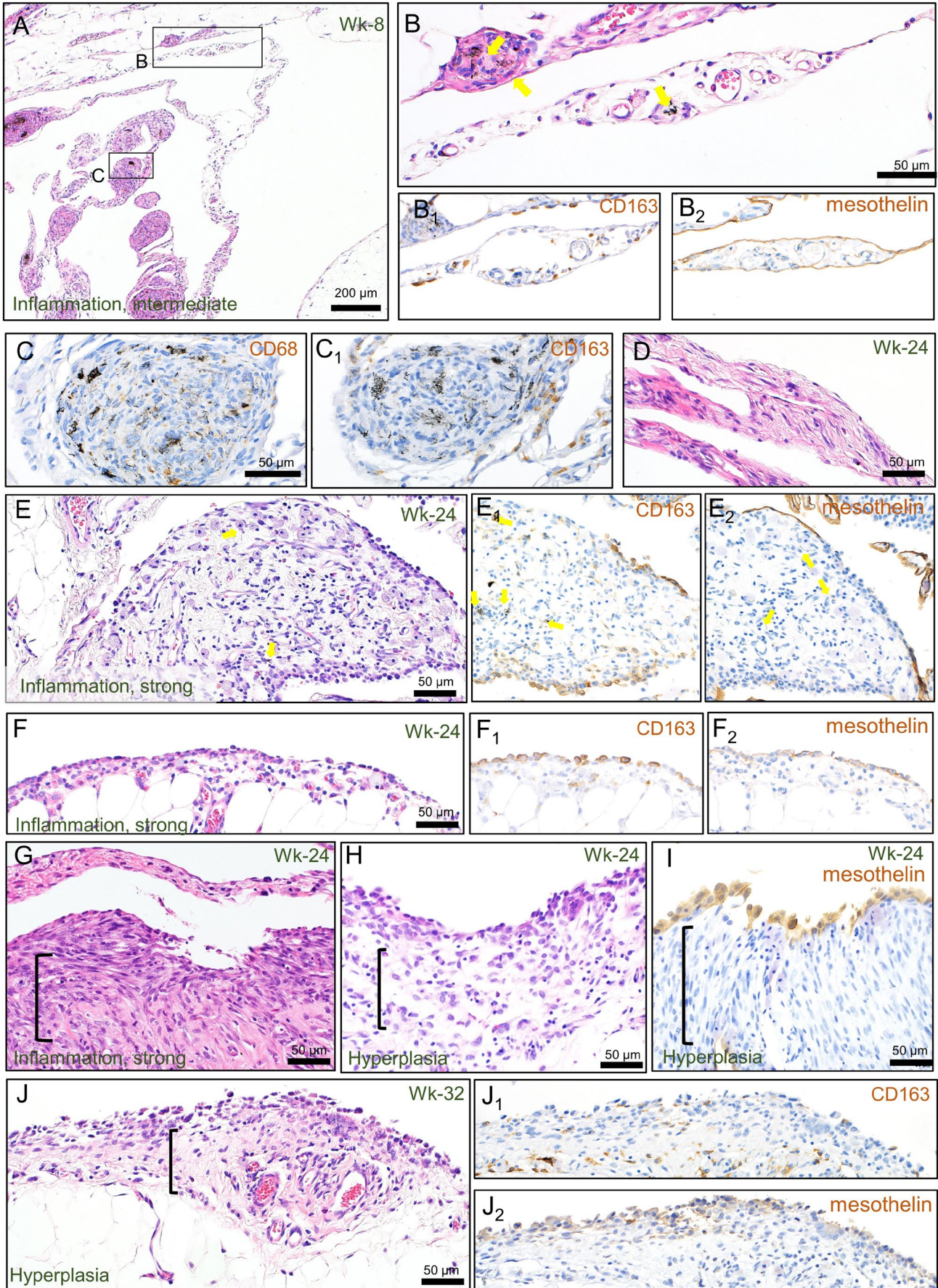


(Table 3 and Figure 1H, I). Hyperplastic lesions were usually accompanied by monocyte deposition (Figure 1J, J₁).

Immunohistochemically, mesothelin signals were confined to the surface of the mesothelium in inflammatory and proliferative lesions (Figure 1B₂, E₂, F₂, I, J₂). CD68-positive cells were mainly observed as MWCNT-laden macrophages in the granulomas and among the lymphocyte infiltrations in the peritoneum (Figure 1C), whereas CD163-positive (Figure 1B₁, E₁, F₁) and CD8-positive (data not shown) cells were distributed widely in the edematous peritoneum. Of note, the location of the CD163 signal at the surface of the mesothelium matched well the site of "monocyte covering" (Figure 1E₁, F₁).

3.2 | Histological characteristics and types/subtypes of the mesothelioma induced by MWCNT

At Wk-24 and Wk-32, the early phase of mesothelioma became recognizable as a small spherical nodule protruding from the inflammatory thickened mesothelium containing free or macrophage-engulfed MWCNT fibers (Figure 2A, B). The nodule consisted of several outer layers of neoplastic cells (Figure 2C), an underlayer of connective tissue-like cells, and a hypocellular core with a large extracellular matrix containing collagen and acid mucopolysaccharides (Figure 2C₁, C₂). The boundary between the neoplastic cells and the underlayer was ambiguous. As seen in inflammatory lesions, CD163-positive (Figure 2C₃) and CD8-positive (data not shown) cells were scattered in the tumor nodule, while CD68-positive cells were rarely found (data not shown). Large parts of the neoplasm were positive immunohistochemically for calretinin, while the outer layers of the mesothelioma cells were positive for mesothelin (Figure 2C₄, C₅). E-cadherin signals were limited to the outermost layer of the neoplastic cells, whereas those of vimentin were detected in both surface and inner-layered neoplastic cells (Figure 2C₆, C₇). These results showed that the mesothelioma should be diagnosed as an epithelioid type, but simultaneously showed mesenchymal features. We called this histological structure "spherical connective tissue rich (SCR)" epithelioid mesothelioma, because it differed from ordinary epithelioid mesothelioma and could not be classified to any subtypes of human MPM.

During the 42-wk observation period, we observed more varying degrees of the mesotheliomas, including more advanced ones (Table 4). In the lower grades, mesothelioma was found as fine nodules with a diameter from 0.1 to 1 mm on the serosa of the fat tissue surrounding the pancreas, a probable primary site. In higher grades, tumors developed large nodules or thick plaques on the

surface of various organs. Invasion was often observed at the diaphragm muscles and the fat tissues in tumor-bearing rats except those in Grade-1. It was also observed at the digestive tract wall and the liver parenchyma, spleen, and kidney in Grade-4 rats. Metastatic cells were found in mediastinal lymph nodes in 6 cases of Grade-2 or higher and in capillary vessels of the lung parenchyma in 2 cases of Grade-4 disease (Table 4 and Figure S3B). Based on the observation of H&E staining, all tumors were classified into 3 histological types and assigned to appropriate subtypes. While most of the Grade-1 cases showed the epithelioid type showing SCR, the Escr subtype, the incidence of the sarcomatoid type increased in the Grade-3 cases and more in Grade-4 cases, in which several types/subtypes often coexisted in the same animal (Table 4). Among various types/subtypes detected in Grade-3 and Grade-4 cases, the solid subtype of the epithelioid type (Esol), the biphasic type (B), and the conventional subtype of the sarcomatoid type (Scon) were the most commonly observed (Table 4 and Figure 2D-F).

3.3 | Time-course of concentrations of humoral factors in the PLF during the early mesotheliomagenesis

To clarify what kinds of molecules were involved in the initiation of mesotheliomagenesis, concentrations of various proteins in the PLF were measured, obtained in Experiment 1. From this observation, levels of almost all factors examined tended to be upregulated in the MWCNT-dosed group. Levels of CINC-1 and CCL2, major chemokines secreted by mesothelial cells, were constantly increased (Figure 3A, B). The level of CCL2, a chemokine that attracts monocytes, peaked at Wk-16, and might be related to monocyte infiltration on the peritoneum surface (Figure 1E and Table 3). Pro-inflammatory and M1 macrophage-related markers, such as IL-1 β and IL-12 (Figure 3C, D), were decreased and slightly raised, respectively. By contrast, TGF- β 1, an anti-inflammatory cytokine and M2 marker, showed constant upregulation and a marked increase at Wk-32 (Figure 3E). Mesothelin/N-ERC, a mesothelioma marker, was largely increased in the MWCNT-dosed groups without a marked elevation or a time-dependent change (Figure 3F). connective tissue growth factor (CTGF), a recently found mesothelioma marker,¹⁶ increased, especially at Wk-16, and seemed to coincide with fibrosis in the peritoneum (Figure 3G and Table 3).

Additionally, Apo A-IV, a components of lipoprotein particles was measured. Compared with the vehicle control, the Apo A-IV level in the PLF significantly decreased in the MWCNT-dosed group at Wk-8, Wk-24, and Wk-32, and showed a time-dependent reduction (Figure 3H).

FIGURE 2 Histological characterization of the mesotheliomas found in Experiment 1. Small nodules of the early phase of mesothelioma found in the fat tissue around the pancreas (A). High-power view of an inflammatory area around deposited MWCNT fibers (B) and their polarized images (B₁ and B₂). High-power view of the tumor nodule (C), Sirius Red staining (C₁), and colloidal iron staining (C₂). Immunohistochemical staining of CD163 (C₃), calretinin (C₄), mesothelin (C₅), E-cadherin (C₆), and vimentin (C₇). Representative histology of advanced mesothelioma cases classified into epithelioid (D), biphasic (E), and sarcomatoid (F) type. Arrows show MWCNT fibers. Esol, solid subtype of the epithelioid mesothelioma; Scon, conventional subtype of sarcomatoid mesothelioma

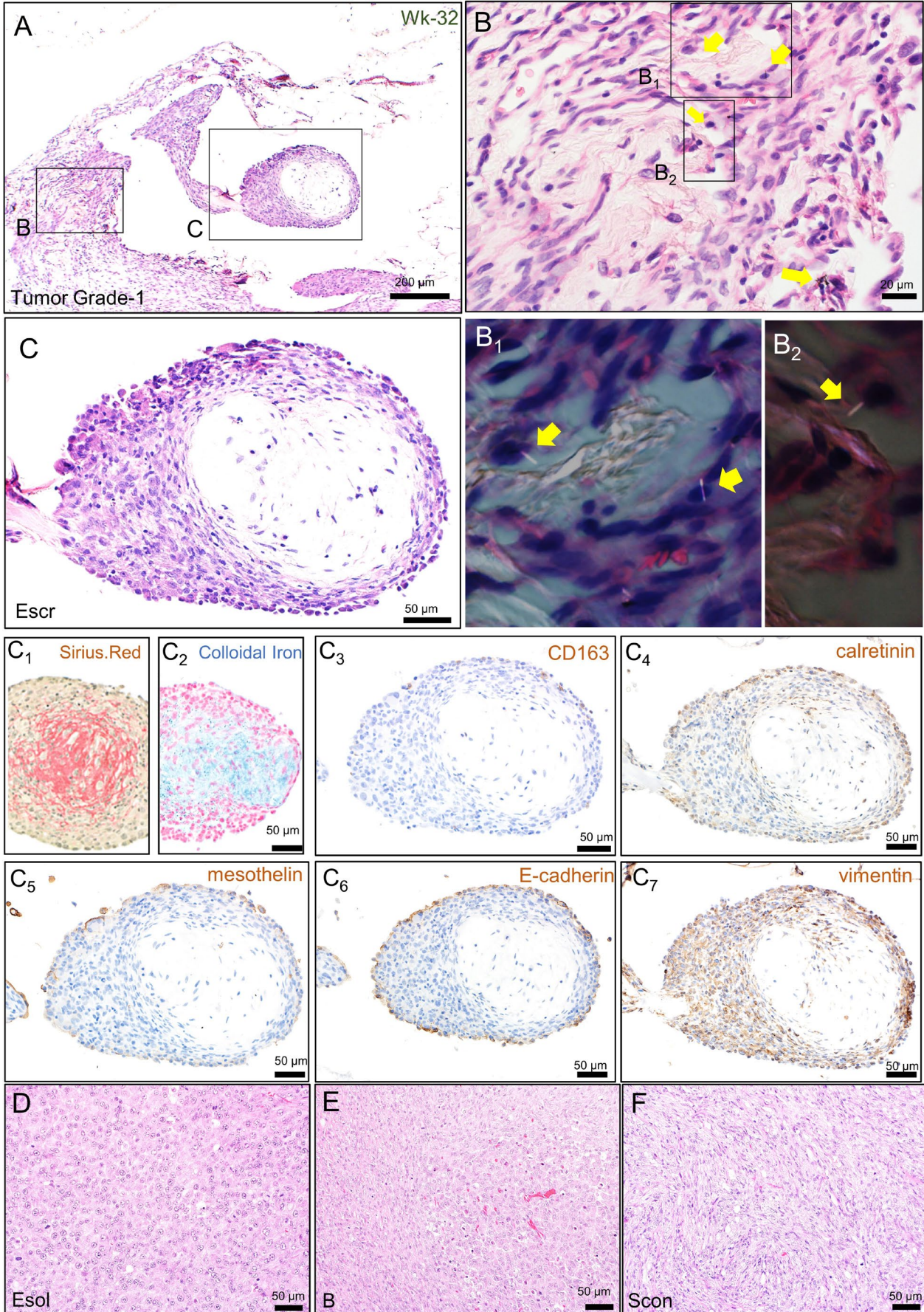


TABLE 4 Individual histopathological data of all rats with mesothelioma in Experiment 1

Grade	Animal number	Necropsy time (weeks after ip)	Type of necropsy	Histological type as an individual	Major subtype	Minor subtype	Vascular invasion, metastasis
Tumor Grade-1	#1-32-1	32	ss	E	Escr	Sost	
	#1-32-11	32	ss	E	Escr		
	#1-32-12	32	ss	E	Escr		
	#1-32-14	32	ss	E	Escr		
	#2-2	42	ss	E	Escr		
	#2-4	42	ss	E	Escr		
Tumor Grade-2	#1-24-3	24	ss	E	Escr		
	#2-11	25	d	E	Erha	Escr	LN
	#1-32-6	32	ss	E	Escr		
	#2-5	42	ss	E	Escr	Scon, B, Esol	LN
Tumor Grade-3	#1-32-7	28	ms	E	Escr	Scon	
	#2-8	41	ms	S	Sost	Scon, B, Escl	LN
	#2-1	42	ss	S	Scon	Escr, Esol, B	
Tumor Grade-4	#2-3	35	ms	S	Scon	B, Esol, Sdes, Esig	V, LN
	#2-10	37	ms	S	Scon	B, Esol, Escl	LN
	#2-6	39	ms	S	Scon	Sple, Escl	
	#2-12	39	d	B	B	Erha, Scon, Esol, Escl	V, LN

Abbreviations: B, biphasic; d, dead; E, epithelioid; Escl, epithelioid tumor showing "spherical connective tissue rich," LN, metastasis in mediastinal lymph node; ms, moribund sacrifice. Other histological subtypes are shown by a rule described in Materials and Methods; S, sarcomatoid; ss, scheduled sacrifice; V, vascular invasion (tumor cells in capillary vessels of the lung parenchyma).

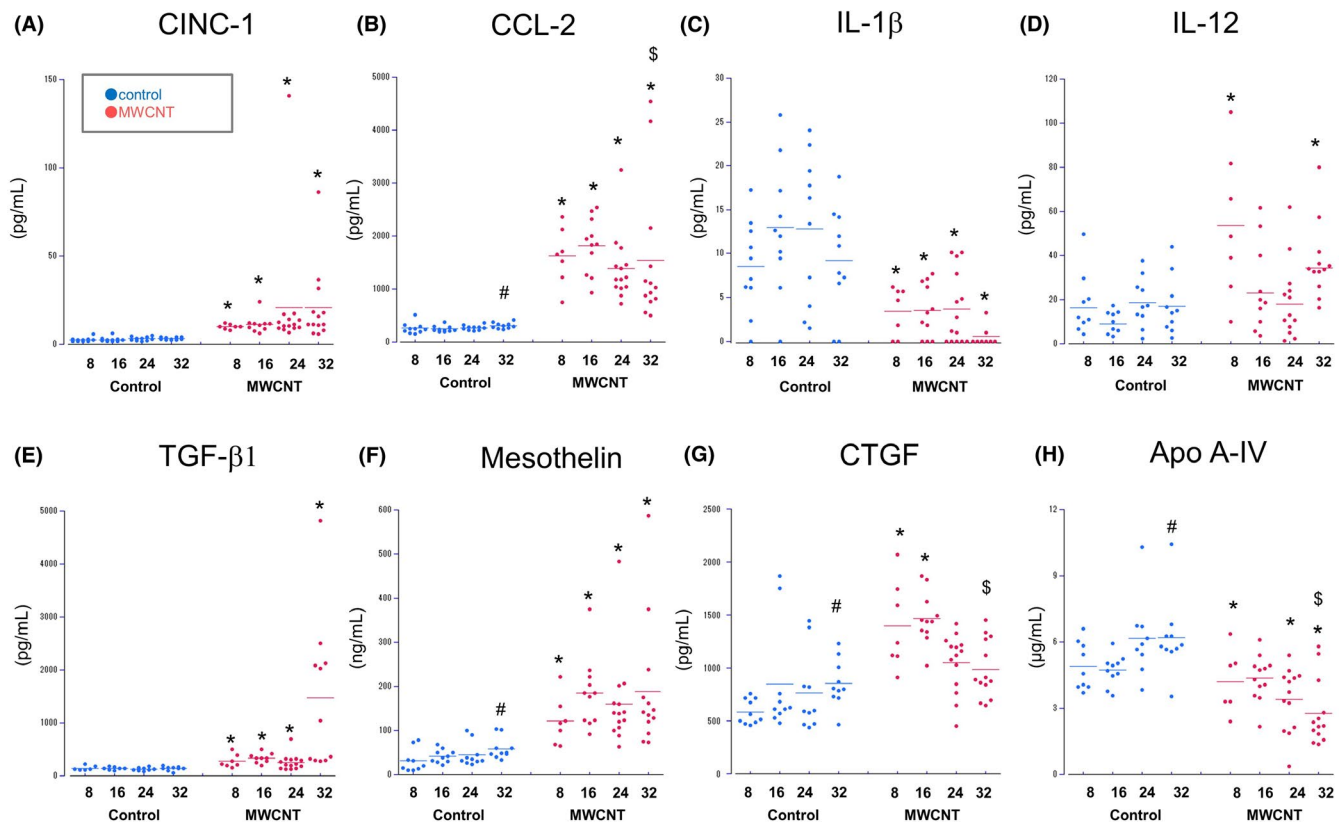


FIGURE 3 Time-course of the levels of humoral factors in the PLF. Scatter plots for CINC-1 (A), CCL-2 (B), IL-1 β (C), IL-12 (D), TGF- β 1 (E), mesothelin/N-ERC (F), CTGF (G) and Apo A-IV (H). Bars show mean values in each time point. Significant changes were denoted by letters: differences between control and dosed groups (*); tendencies of increase (#) or decrease (\$) from Wk-8 to Wk-32

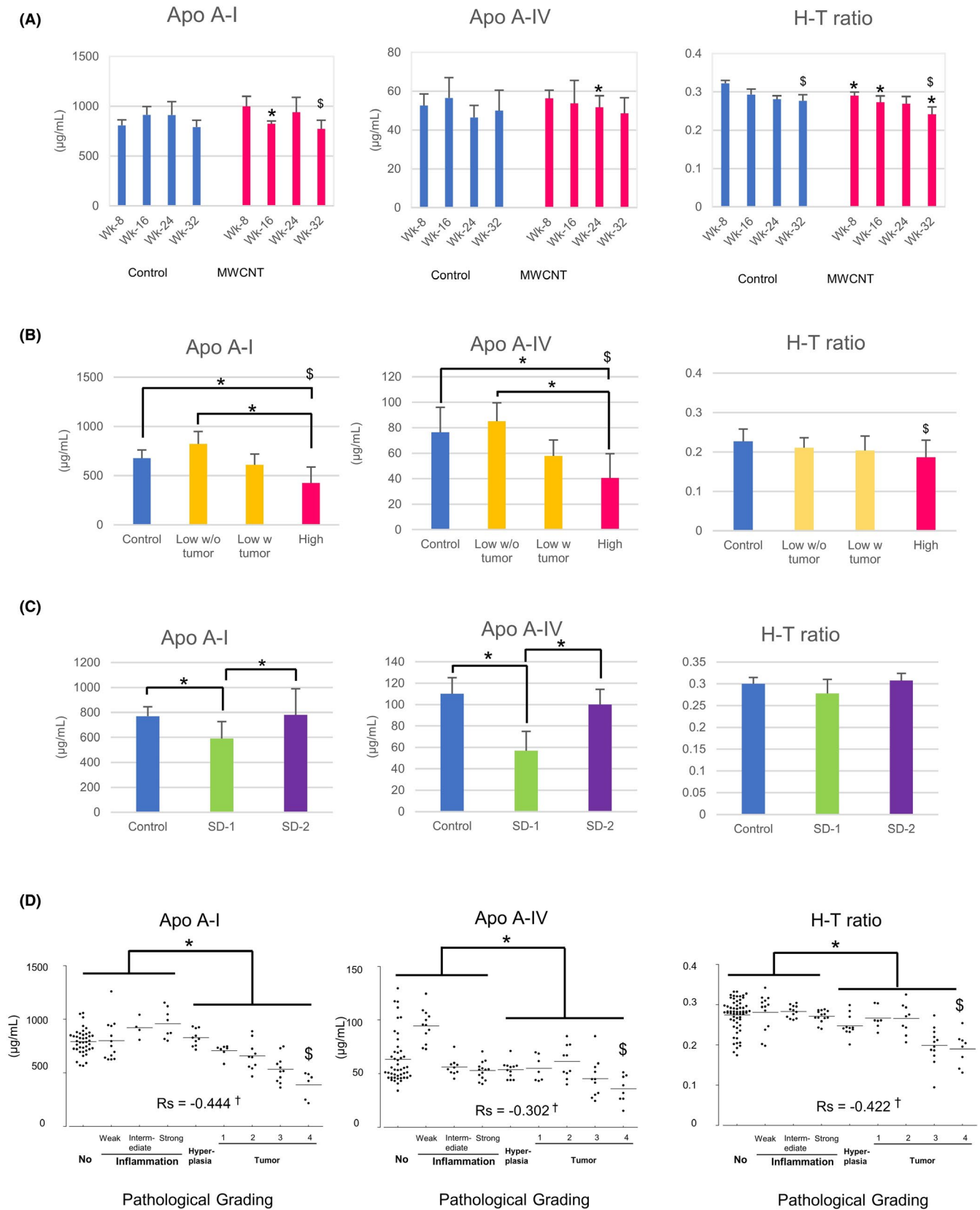


FIGURE 4 Serum levels of apolipoproteins and cholesterols. Mean values with standard deviations of Apo A-I, Apo A-IV, and H-T ratio in Experiment 1 (time-course analysis) (A), Experiment 2 (dose-dependent carcinogenicity) (B), and Experiment 3 (different types of MWCNTs) (C). Scatter plots of integrated data of the 3 experiments (D). Bars show mean values. Rs: Spearman Rho value. Significant changes were denoted by letters: differences between the 2 groups (*); tendencies of decrease (§) with a time-dependency (A), a tumor burden (B), and a histological grading (D); correlation of the lipoprotein-related parameters and the pathological grading (†)

3.4 | Serum levels of lipoprotein and cholesterol in the MWCNT-dosed rat

To investigate the relationship between the serum levels of lipoprotein-related molecules and mesothelioma pathological change, we used more samples from 2 carcinogenicity tests, Experiments 2 and 3. In Experiment 2, the rats were dosed with 2 different doses of Taq-MWNT-7. The results of the tumor incidences and survival rates showed a dose-dependent signature (Table S3). Compared with the original MWNT-7, Taq-MWNT-7 induced less granuloma formation in the peritoneum (detailed results are shown in Figure S4) that was unrelated to the tumor incidence, at least at a dose of 1 mg/kg BW (100%). On the other hand, in Experiment 3, the SD-1, a thick, long fiber, induced mesothelioma in 100% of rats, while the SD-2, a thin, tangled fiber, did not induce any proliferative lesions (Table S4). The SD-2 fibers were observed in large granulomas or the macrophages within the peritoneal lymphatic infiltration (Figure S3A, arrow). We obtained 110 samples with a wide range of pathological grades from these 2 experiments, as shown in Tables S3 and S4. Similar to the result of Experiment 1, advanced mesotheliomas showed various histological features (Figure S5). Metastases often occurred in the mediastinal lymph node and a few high-graded cases in the lung were seen (Figure S3B).

Using all available serum samples from the 3 experiments, we then examined serum levels of Apo A-I (another major component of lipoproteins), Apo A-IV, total cholesterol, HDL cholesterol, LDL cholesterol, and triglyceride. In Experiment 1, the serum levels of Apo A-I, Apo A-IV, or a ratio of HDL cholesterol and total cholesterol (H-T ratio) tended to decrease in the MWCNT-dosed group in

a time-dependent manner (Figure 4A). In Experiment 2, sera from the vehicle control group, and the low or high doses of Taq-MWNT-7 exposed groups were analyzed. The levels of Apo A-I, Apo A-IV, and the H-T ratio gradually decreased in the following order: vehicle > low-dose without tumor > low-dose with tumor > high-dose (Figure 4B). By contrast, LDL cholesterol and the ratio of LDL cholesterol and total cholesterol (L-T ratio) increased depending on the morbidity and the dosage (Figure S6). In Experiment 3, the concentrations of Apo A-I and A-IV proteins were significantly lower in the SD-1-dosed group compared with the vehicle control and the SD-2 dosed group (Figure 4C).

When all data were reconstructed in accordance with the pathological grading (Table 1; using the Total Consecutive Grade, 9-grading, 0-8), the serum levels of Apo A-I, Apo A-IV, and H-T ratio were found to be negatively correlated with the grading individually, while the LDL cholesterol or L-T ratio was positively correlated with the grading (Figures 4D and S6 and Table S5). The degree of correlation was more marked when focusing on the rats with proliferative lesions compared with those without (Table S5, the right-most column; using only 4-8 of the Total Consecutive Grade; Hyperplasia and Tumor Grades-1, 2, 3, and 4 [therefore, 5-grading]). For a comparison, mesothelin/N-ERC was measured in the same samples, and a positive correlation with the pathological grading was confirmed (Figure S6).

Results of immunohistochemistry and quantitative RT-PCR revealed no substantial decrease in the production of Apo A-I and A-IV in the intestine and the liver (major apolipoprotein-producing tissues) of the tumor-bearing rats (Figures S7 and S8). In addition, in the mesothelioma tissues, prominent depositions of these apolipoproteins were observed. Immunohistochemical signals were observed in the

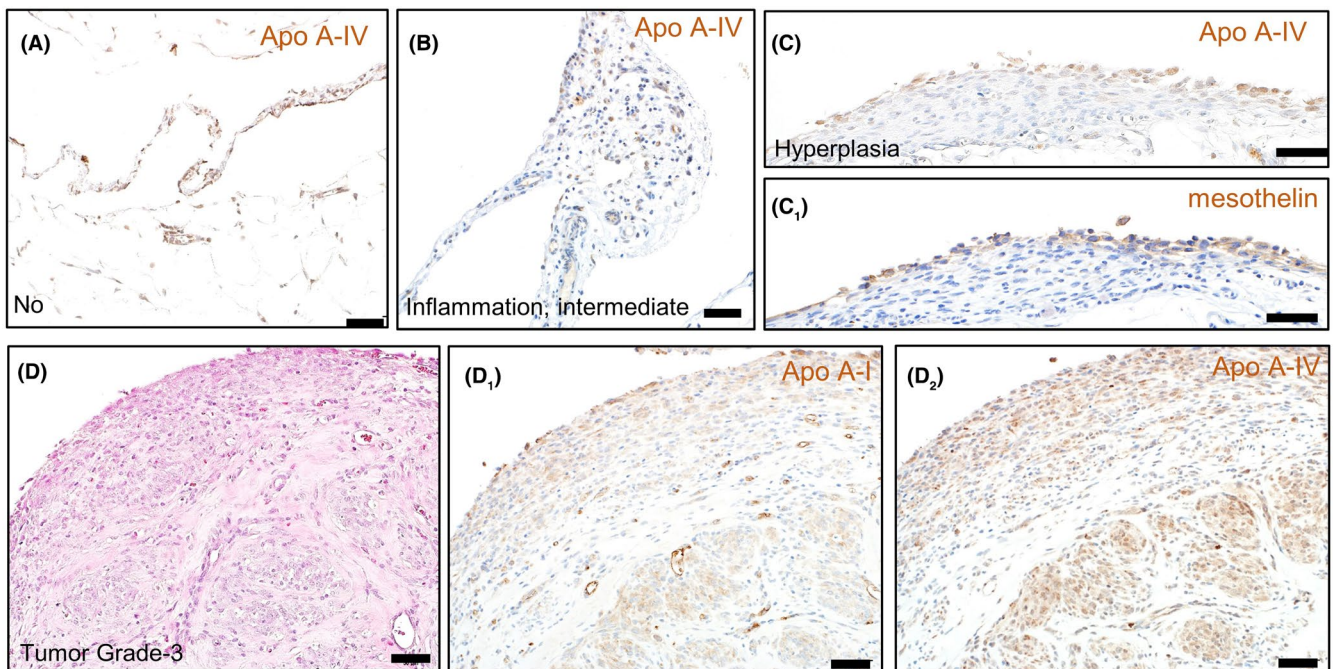


FIGURE 5 Localization of apolipoproteins in the mesothelium. Immunohistochemical staining of Apo A-IV in the intact mesothelium (A), inflammatory lesion (B), hyperplasia (C), and mesothelioma (D₂). Immunohistochemical staining of mesothelin (C₁) or Apo A-I (D₁). A H&E image of the serial section (D)

mesothelial cells and within the microvessels in the intact mesothelium or the inflammatory lesion (Figure 5A, B). From hyperplasia to advanced mesotheliomas, the apolipoproteins were mainly localized to proliferating mesothelial cells (Figure 5C, D). They appeared to be supplied by the blood because their gene expression levels were much lower in the tumor nodules, compared with those from the liver and intestine (Figure S8). There was no relationship between the deposition of apolipoproteins and the infiltration pattern of immune cells in large tumor nodules (Figure S9).

4 | DISCUSSION

Our time-course analysis demonstrated that the MWCNT fibers certainly induced a chronic inflammation on the abdominal serosal surface, lasting for 32 wk with a tendency to gradually subside. The preferential localization of granulomas or early mesotheliomas at the rostral region of the coelom suggested that the MWCNT fibers tended to accumulate via the lymphatic fluid. As described in Donaldson "stoma theory", fibrous particles with a high aspect ratio could not move to small pores of the parietal pleura (the lymphatic stoma) and evoke inflammation.¹⁷ In this study, the MWCNT fibers were presumably trapped at the stomata of the mesothelium of the diaphragm or serosa of the peritoneal organs. Even though the majority of the fibers were embedded in granulomas and fibrous scars, considerable numbers of singlet fibers remaining in the peritoneum continued to provoke inflammation on the mesothelium surface and induce a focal regenerative response. Accordingly, the levels of the 2 chemokines were always high in the dosed group. Given that mesothelial tissue repair is usually completed by 1 wk after the injury,^{18,19} frequent repetition of mesothelial injury and regeneration was supposed to occur by Wk-24. It is plausible that mesothelial cells might have been exposed to genomic insults during this period.

In addition to showing chronic inflammation, our data suggested that anti-inflammatory conditions could be related to the beginning of mesotheliomagenesis. If the peritoneal mesothelium is histologically examined soon after exposure, infiltrations of CD68-positive macrophages engulfing MWCNTs and neutrophils were significant findings (24-48 h after injection; our unpublished data). By contrast, 8 wk after injection, infiltrations of non-phagocytic macrophages, eosinophils, and lymphocytes were predominant, and fibrosis and granulation occurred. Although pro-inflammatory cytokines such as IL-1 β and IL-12 were not, or only slightly upregulated, the level of TGF- β was constantly high with a marked elevation in Wk-32. TGF- β contributes to the tissue repair process by regulating myofibroblast differentiation, collagen deposition, and scar formation. It is also known to be a key mediator released by immunosuppressive cells such as T-regs and myeloid-derived suppressor cells. Therefore, our results seemed to support the view that nanoparticle-related carcinogenesis occurs in the immunosuppressive condition after the inflammatory state, rather than through solely unresolved inflammation²⁰

The M2 monocyte/macrophage lineage is generally thought to be involved in tissue repair, as well as tumorigenesis. In this study,

the milieu of the peritoneum seemed to be polarized to M2 before the initiation of mesothelioma. CD163-positive cells were observed at the surface area of the regenerative and proliferating mesothelium and the stroma of the advanced tumor. These cells were probably recruited by the CCL2/CCR2 pathway because of the agreement between histological findings and CCL2 levels in the PLF. Several authors have reported populations of macrophages on the surface of injured peritoneum of rats,^{19,21,22} in which macrophages may play a role in enhancing the proliferation of mesothelial cells.²³ As seen in other cancers, M2-related macrophages, such as tumor-associated macrophages, contribute to the malignancy of human MPM.^{24,25} For instance, the level of tumor-infiltrated CD163-positive macrophages is positively correlated with CCL2 concentration in the pleural effusion of MPM patients and was related to a poor prognosis.²⁶ Flow cytometric analysis showed that monocyte-derived immunosuppressive cells were recruited to the peritoneal cavity of rats by a CCL2/CCR2 pathway after an injection of MWNT-7.²⁷ Therefore, our constant findings of CD163-positive cells in the vicinity of mesothelial cells may indicate their continuous involvement in these pathological contexts.

Histologically, the first manifestation of the preneoplastic condition was the hyperplasia composed of atypical polygonal cells on the mesothelium surface associated with inflammatory cells. These findings agree with those of atypical hyperplasia in *p53*-heterozygously knocked-out mice in which bulging of cuboidal or hobnail-shaped mesothelial cells was observed near an accumulation of inflammatory cells, especially lymphocytes and macrophages-like cells.⁹ In our study, SCR mesothelioma was a major subtype emerging at the beginning of tumorigenesis. The SCR-like structure has been reported in the other publications on mesotheliomas induced by MWCNT in rats or *p53*-heterozygously knocked-out mice.^{27,28} The submesothelial fibroblast-like multipotent cell is thought to be a major source of new mesothelial cells during wound healing.^{19,29} Similarly, the fibroblast-like cells found in the early neoplastic lesions may actively produce mesothelial cells externally, while the mesothelial cell-secreting hyaluronan-like matrix can become the core of the nodule. By contrast, the connective tissue-like area also appeared to be a "transitional" type mesothelioma (between epithelioid and sarcomatoid mesothelioma).^{30,31} It is possible that epithelioid type cells on the surface expand beneath the mesothelium via the epithelial-mesenchymal transition-like phenomenon.^{32,33} Fujii et al demonstrated that crosstalk between TGF- β and Hippo signaling induced expression of CTGF, which plays essential roles in mesothelioma progression (eg, cell growth, deposition of extracellular matrix, and histological transition from epithelioid type to sarcomatoid type).^{16,34} In our time-course analysis, levels of TGF- β and CTGF increased in the PLF; this was perhaps related to the growth of connective tissue-like cells in the early mesothelioma and tumor progression. However, the cell type composition in the connective tissue-like area remains elusive.

The histological classification of the rat mesothelioma induced by MWCNT has not been well discussed. Rittinghausen et al analyzed 329 rat peritoneal mesotheliomas and pointed out that the tumors that differentiated to sarcomatoid types were more preferentially compared with epithelioid or biphasic types.³⁵ Although our results

also showed a slight tendency to become sarcomatous in advanced cases, the total incidence of the sarcomatoid type was similar to that of the epithelioid type, when the results from Experiments 1 to 3 were combined (data not shown). Furthermore, in the 2 carcinogenic experiments, a difference in the predominant histological type (epithelioid, biphasic, or sarcomatoid) was not relevant to either the survival time, the occurrence of metastasis, or serum levels of mesothelin- or lipoprotein-related molecules (data not shown). In the present study, we found versatile subtypes of mesotheliomas, but rarely encountered the papillary proliferation of the neoplastic cells that is a major histological pattern in human MPM. This finding contrasts with the rat spontaneous mesothelioma and the mesotheliomas induced by repeated injection of asbestos or iron overload.^{16,36} An aggressive and wide-spectrum attack on the peritoneal mesothelium, probably as a result of MWCNT's physical properties (eg, high surface area, rigidity and high aspect ratio), seems to be related to the high incidence of mesothelioma in a short period. This condition, perhaps, prevents the mesothelioma from forming the papillary structure. We showed that the MWCNT-induced mesotheliomas showed various histological subtypes such as signet ring, pleomorphic, rhabdoid structures in advanced cases, similar to human MPM. This information may provide basic knowledge to exploit the rat model for a more detailed histological analysis. However, it was difficult to evaluate the subtypes' relevance for other tumor biological parameters such as survival rate or metastasis because the numbers of each subtype were not sufficient for comparative analysis and several subtypes arose simultaneously in 1 animal.

We revealed a notable change in the serum levels of lipoprotein and cholesterol during the development of mesothelioma. Dysregulation of lipid metabolism in cancer pathogenesis and cholesterol-lowering therapy have been known in various types of cancers. Recent studies have demonstrated a positive correlation

between LDL cholesterol level and breast cancer risk, but a negative correlation between HDL cholesterol level and the cancer risk.³⁷ We speculated that the decline the serum lipoprotein-related parameters may result from the progression of the mesothelioma. For example, the synthesis of cholesterol in the liver and intestine and its subsequent transport cannot meet the demands of growing tumor cells required to maintain cell membranes and the modulation of membrane fluidity, leading to a substantial decline in cholesterol in the blood pool. This lipid homeostasis was reported in colorectal cancer.^{38,39} Furthermore, malignant neoplasms generally cause malnutrition and cachexia. Our results probably show one of the systemic metabolic changes that are common in advanced cancers. Alternatively, the results could be interpreted to mean that a low supply of apolipoproteins/HDL cholesterol to the neoplastic tissue may cause mesothelioma exacerbation. A growing body of evidence has revealed that apolipoproteins/HDL cholesterol may play a role in antioxidant response, anti-inflammatory activity, and tumor immunity, reducing the risk of malignancy of tumors.⁴⁰⁻⁴² For instance, a recombinant Apo A-IV has been shown to mitigate inflammation in experimental colitis.⁴³ In vivo studies using transgenic and knockout mice showed that Apo A-I drastically prompts inoculated melanoma and ovarian cancer regression by the modulation of immune responses.^{44,45} In this study, however, we could not find any suggestive immune signatures, such that a favorable infiltration of antitumor CD8-positive cells and/or an elimination of M2 macrophages tended to occur in the tumor tissue with a marked deposition of apolipoproteins. Therefore, the former scenario is more plausible. Our results suggest that mesothelioma also has to be added to the list of cancers, of which the pathogenesis involves the imbalance of lipoproteins. The serum level of Apo As, for instance, could potentially apply to the staging of MPM patients. To our knowledge, a few proteomic analyses have shown declines of

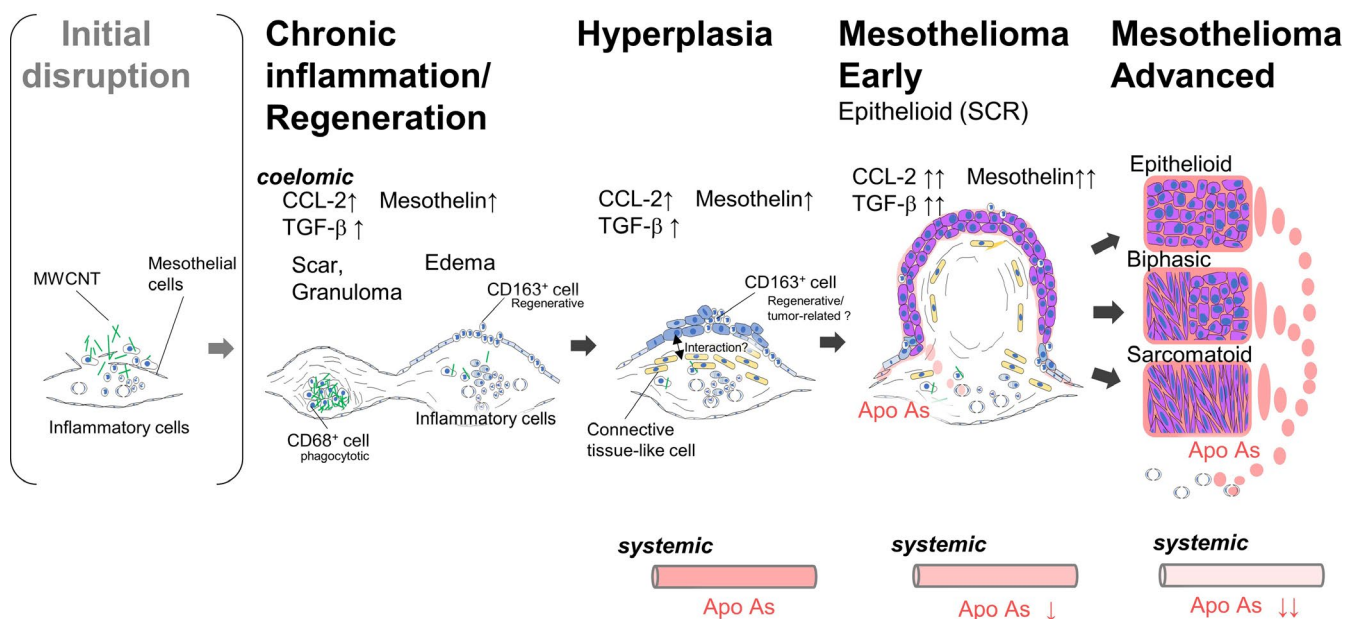


FIGURE 6 Scheme of the sequence of the development of rat mesothelioma by MWCNT in this study

apolipoproteins A-I, A-II, or C-I in the sera or pleural effusions of the MPM patients.^{46,47} Further clinical studies are needed to determine whether the apolipoproteins are associated with human MPM development and are useful as therapeutic targets.

In conclusion, MWCNT-related mesothelioma is developed under chronic inflammation and the repetitive regenerations in which M2 monocytes are involved. As the tumor progresses, the histological feature of the mesothelioma changed from a distinct epithelioid subtype, SCR, to versatile histological patterns including sarcomatous types (Figure 6). The tumor grade was negatively correlated to serum levels of apolipoproteins and HDL cholesterol content.

ACKNOWLEDGMENTS

We thank Professor Hiroyuki Tsuda, Dr. Takamasa Numano, and Dr. Akio Ogata for helpful discussion, and Katsuhiko Yuzawa, Yuko Hasegawa, Norio Yano, Akemichi Nagasawa, the late Yoshikazu Kubo, Fujifumi Kaihoko, Hiroshi Ando, and Kazuyoshi Tanaka for their superb technical support. This study was supported by Health and Labour Sciences Research Grants (H27-Kagaku-Shitei-004 and H30-Kagaku-Shitei-004) from the Ministry of Health, Labour and Welfare, Japan.

DISCLOSURE

The authors have no conflicts of interest.

ORCID

Motoki Hojo  <https://orcid.org/0000-0001-5386-5110>

Dai Nakae  <https://orcid.org/0000-0001-5895-3830>

REFERENCES

- Kasai T, Umeda Y, Ohnishi M, et al. Lung carcinogenicity of inhaled multi-walled carbon nanotube in rats. *Part Fibre Toxicol.* 2016;13:53.
- Pauluhn J. Subchronic 13-week inhalation exposure of rats to multiwalled carbon nanotubes: toxic effects are determined by density of agglomerate structures, not fibrillar structures. *Toxicol Sci.* 2010;113:226-242.
- Mercer RR, Hubbs AF, Scabilloni JF, et al. Pulmonary fibrotic response to aspiration of multi-walled carbon nanotubes. *Part Fibre Toxicol.* 2011;8:21.
- Suzui M, Futakuchi M, Fukamachi K, et al. Multiwalled carbon nanotubes intratracheally instilled into the rat lung induce development of pleural malignant mesothelioma and lung tumors. *Cancer Sci.* 2016;107:924-935.
- Sakamoto Y, Nakae D, Fukumori N, et al. Induction of mesothelioma by a single intrascrotal administration of multi-wall carbon nanotube in intact male Fischer 344 rats. *J Toxicol Sci.* 2009;34:65-76.
- Takagi A, Hirose A, Nishimura T, et al. Induction of mesothelioma in p53^{+/−} mouse by intraperitoneal application of multi-wall carbon nanotube. *J Toxicol Sci.* 2008;33:105-116.
- Numano T, Higuchi H, Alexander DB, et al. MWCNT-7 administered to the lung by intratracheal instillation induces development of pleural mesothelioma in F344 rats. *Cancer Sci.* 2019;110:2485-2492.
- Hu Q, Akatsuka S, Yamashita Y, et al. Homozygous deletion of CDKN2A/2B is a hallmark of iron-induced high-grade rat mesothelioma. *Lab Invest.* 2010;90:360-373.
- Nagai H, Okazaki Y, Chew SH, et al. Diameter and rigidity of multiwalled carbon nanotubes are critical factors in mesothelial injury and carcinogenesis. *Proc Natl Acad Sci U S A.* 2011;108:E1330-1338.
- Murphy FA, Schinwald A, Poland CA, Donaldson K. The mechanism of pleural inflammation by long carbon nanotubes: interaction of long fibres with macrophages stimulates them to amplify pro-inflammatory responses in mesothelial cells. *Part Fibre Toxicol.* 2012;9:8.
- Chernova T, Murphy FA, Galavotti S, et al. Long-Fiber Carbon Nanotubes Replicate Asbestos-Induced Mesothelioma with Disruption of the Tumor Suppressor Gene Cdkn2a (Ink4a/Arf). *Curr Biol.* 2017;27(3302-3314):e3306.
- Taquahashi Y, Ogawa Y, Takagi A, Tsuji M, Morita K, Kanno J. Improved dispersion method of multi-wall carbon nanotube for inhalation toxicity studies of experimental animals. *J Toxicol Sci.* 2013;38:619-628.
- Sakamoto Y, Hojo M, Kosugi Y, et al. Comparative study for carcinogenicity of 7 different multi-wall carbon nanotubes with different physicochemical characteristics by a single intraperitoneal injection in male Fischer 344 rats. *J Toxicol Sci.* 2018;43:587-600.
- Allen TC. Recognition of histopathologic patterns of diffuse malignant mesothelioma in differential diagnosis of pleural biopsies. *Arch Pathol Lab Med.* 2005;129:1415-1420.
- Husain AN, Colby TV, Ordonez NG, et al. Guidelines for Pathologic Diagnosis of Malignant Mesothelioma 2017 Update of the Consensus Statement From the International Mesothelioma Interest Group. *Arch Pathol Lab Med.* 2018;142:89-108.
- Jiang L, Yamashita Y, Chew SH, et al. Connective tissue growth factor and beta-catenin constitute an autocrine loop for activation in rat sarcomatoid mesothelioma. *J Pathol.* 2014;233:402-414.
- Donaldson K, Murphy FA, Duffin R, Poland CA. Asbestos, carbon nanotubes and the pleural mesothelium: a review of the hypothesis regarding the role of long fibre retention in the parietal pleura, inflammation and mesothelioma. *Part Fibre Toxicol.* 2010;7:5.
- Rafferty AT. Regeneration of parietal and visceral peritoneum in the immature animal: a light and electron microscopical study. *Br J Surg.* 1973;60:969-975.
- Rafferty AT. Regeneration of parietal and visceral peritoneum: an electron microscopical study. *J Anat.* 1973;115:375-392.
- Huax F. Emerging Role of Immunosuppression in Diseases Induced by Micro- and Nano-Particles: Time to Revisit the Exclusive Inflammatory Scenario. *Front Immunol.* 2018;9:2364.
- Nishioka Y, Miyazaki M, Abe K, et al. Regeneration of peritoneal mesothelium in a rat model of peritoneal fibrosis. *Ren Fail.* 2008;30:97-105.
- Teranishi S, Sakaguchi M, Itaya H. Mesothelial regeneration in the rat and effect of urokinase. *Nihon Geka Hokan.* 1977;46:361-379.
- Mutsaers SE, Whitaker D, Papadimitriou JM. Stimulation of mesothelial cell proliferation by exudate macrophages enhances serosal wound healing in a murine model. *Am J Pathol.* 2002;160:681-692.
- Ujii H, Kadota K, Nitadori JI, et al. The tumoral and stromal immune microenvironment in malignant pleural mesothelioma: A comprehensive analysis reveals prognostic immune markers. *Oncoimmunology.* 2015;4:e1009285.
- Cornelissen R, Lievens LA, Maat AP, et al. Ratio of intratumoral macrophage phenotypes is a prognostic factor in epithelioid malignant pleural mesothelioma. *PLoS One.* 2014;9:e106742.
- Chene AL, d'Almeida S, Blondy T, et al. Pleural Effusions from Patients with Mesothelioma Induce Recruitment of Monocytes and Their Differentiation into M2 Macrophages. *J Thorac Oncol.* 2016;11:1765-1773.
- Huax F, d'Ursel de Bousies V, Parent MA, et al. Mesothelioma response to carbon nanotubes is associated with an early and selective accumulation of immunosuppressive monocytic cells. *Part Fibre Toxicol.* 2016;13:46.
- Takagi A, Hirose A, Futakuchi M, Tsuda H, Kanno J. Dose-dependent mesothelioma induction by intraperitoneal administration of multi-wall carbon nanotubes in p53 heterozygous mice. *Cancer Sci.* 2012;103:1440-1444.

29. Mutsaers SE. Mesothelial cells: their structure, function and role in serosal repair. *Respirology*. 2002;7:171-191.
30. Travis WD, International Agency for Research on C. *WHO classification of tumours of the lung, pleura, thymus and heart.*, 4th edn. International Agency for Research on Cancer; 2015:412 p.
31. Galateau Salle F, Le Stang N, Nicholson AG, et al. New Insights on Diagnostic Reproducibility of Biphasic Mesotheliomas: A Multi-Institutional Evaluation by the International Mesothelioma Panel From the MESOPATH Reference Center. *J Thorac Oncol*. 2018;13:1189-1203.
32. Turini S, Bergandi L, Gazzano E, Prato M, Aldieri E. Epithelial to Mesenchymal Transition in Human Mesothelial Cells Exposed to Asbestos Fibers: Role of TGF-beta as Mediator of Malignant Mesothelioma Development or Metastasis via EMT Event. *Int J Mol Sci*. 2019;20.
33. Sandoval P, Loureiro J, Gonzalez-Mateo G, et al. PPAR-gamma agonist rosiglitazone protects peritoneal membrane from dialysis fluid-induced damage. *Lab Invest*. 2010;90:1517-1532.
34. Fujii M, Toyoda T, Nakanishi H, et al. TGF-beta synergizes with defects in the Hippo pathway to stimulate human malignant mesothelioma growth. *J Exp Med*. 2012;209:479-494.
35. Rittinghausen S, Hackbarth A, Creutzenberg O, et al. The carcinogenic effect of various multi-walled carbon nanotubes (MWCNTs) after intraperitoneal injection in rats. *Part Fibre Toxicol*. 2014;11:59.
36. Jiang L, Akatsuka S, Nagai H, et al. Iron overload signature in chrysotile-induced malignant mesothelioma. *J Pathol*. 2012;228:366-377.
37. Ni H, Liu H, Gao R. Serum Lipids and Breast Cancer Risk: A Meta-Analysis of Prospective Cohort Studies. *PLoS One*. 2015;10:e0142669.
38. Zhang X, Zhao XW, Liu DB, et al. Lipid levels in serum and cancerous tissues of colorectal cancer patients. *World J Gastroenterol*. 2014;20:8646-8652.
39. Dessi S, Batetta B, Pulisci D, et al. Cholesterol content in tumor tissues is inversely associated with high-density lipoprotein cholesterol in serum in patients with gastrointestinal cancer. *Cancer*. 1994;73:253-258.
40. Zamanian-Daryoush M, DiDonato JA. Apolipoprotein A-I and Cancer. *Front Pharmacol*. 2015;6:265.
41. Spaulding HL, Saijo F, Turnage RH, Alexander JS, Aw TY, Kalogeris TJ. Apolipoprotein A-IV attenuates oxidant-induced apoptosis in mitotic competent, undifferentiated cells by modulating intracellular glutathione redox balance. *Am J Physiol Cell Physiol*. 2006;290:C95-C103.
42. Wang Y, Sun XQ, Lin HC, et al. Correlation between immune signature and high-density lipoprotein cholesterol level in stage II/III colorectal cancer. *Cancer Med*. 2019;8:1209-1217.
43. Vowinkel T, Mori M, Krieglstein CF, et al. Apolipoprotein A-IV inhibits experimental colitis. *J Clin Invest*. 2004;114:260-269.
44. Zamanian-Daryoush M, Lindner D, Tallant TC, et al. The cardioprotective protein apolipoprotein A1 promotes potent anti-tumorigenic effects. *J Biol Chem*. 2013;288:21237-21252.
45. Su F, Kozak KR, Imaizumi S, et al. Apolipoprotein A-I (apoA-I) and apoA-I mimetic peptides inhibit tumor development in a mouse model of ovarian cancer. *Proc Natl Acad Sci U S A*. 2010;107:19997-20002.
46. Hegmans JP, Veltman JD, Fung ET, et al. Protein profiling of pleural effusions to identify malignant pleural mesothelioma using SELDI-TOF MS. *Technol Cancer Res Treat*. 2009;8:323-332.
47. Ostroff RM, Mehan MR, Stewart A, et al. Early detection of malignant pleural mesothelioma in asbestos-exposed individuals with a noninvasive proteomics-based surveillance tool. *PLoS One*. 2012;7:e46091.

SUPPORTING INFORMATION

Additional supporting information may be found online in the Supporting Information section.

How to cite this article: Hojo M, Yamamoto Y, Sakamoto Y, et al. Histological sequence of the development of rat mesothelioma by MWCNT, with the involvement of apolipoproteins. *Cancer Sci*. 2021;112:2185-2198. <https://doi.org/10.1111/cas.14873>